JOURNAL OF PROPULSION AND POWER
Vol. 12, No. 2, March–April 1996

Crossflow Mixing of Noncircular Jets

D. S. Liscinsky* and B. True†
United Technologies Research Center, East Hartford, Connecticut 06108
and
J. D. Holdeman‡
NASA Lewis Research Center, Cleveland, Ohio 44135

An experimental investigation has been conducted of the isothermal mixing of a turbulent jet injected perpendicular to a uniform crossflow through several different types of sharp-edged orifices. Jet penetration and mixing was studied using planar Mie scattering to measure time-averaged mixture fraction distributions of circular, square, elliptical, and rectangular orifices of equal geometric area injected into a constant velocity crossflow. Hot-wire anemometry was also used to measure streamwise turbulence intensity distributions at several downstream planes. Mixing effectiveness was determined using 1) a spatial unmixedness parameter based on the variance of the mean jet concentration distributions and 2) by direct comparison of the planar distributions of concentration and of turbulence intensity. No significant difference in mixing performance was observed for the six configurations based on comparison of the mean properties.

Nomenclature

A_j = orifice area
A_m = cross-sectional area of mainstream duct at injection location
AR = orifice aspect ratio, L/W
C_{av} = $(m_j/m_m)/(1 + m_j/m_m)$
C_d = orifice discharge coefficient
d = orifice diameter
J = jet-to-mainstream momentum-flux ratio, $(\rho_j V_j^2)/(\rho_m U_{main}^2)$
L = long dimension of orifice
m_j = mass flow of the jet
m_m = mass flow of the mainstream
U_{main} = mainstream velocity
U_s = spatial unmixedness parameter, Eq. (2)
W = short dimension of orifice
x = downstream coordinate, 0 at the leading edge of the orifice
y = cross-stream coordinate, horizontal
z = cross-stream coordinate, vertical
α = angle between longest dimension of orifice and axial direction
ρ_j = density of the jet
ρ_m = density of the mainstream

Introduction

CROSSFLOW mixing is employed in many applications. Generally the objective is to rapidly obtain a homogeneous mixture of the injectant and mainstream. The degree and rate of the mixing process are especially important in combustion applications since burning efficiency and exhaust composition directly depend on mass transfer and reaction kinetics. Whereas kinetics are difficult to control, the mixing process is easily affected by any number of parameters and optimization of that process for combustor design has been the topic of several recent investigations.[1–19]

The use of orifice shape to passively control the mixing process has been studied in nonreacting and reacting systems, and the ability of noncircular, low AR orifices to augment mixing rates in these systems has been demonstrated.[20–24] The increased mixing rate is attributed to a generation of scales, which are smaller than those created by round/circular shapes. The result is increased mixing on a molecular scale that increases reaction rate. Most previous studies of noncircular orifices use nozzles to generate inlet boundary conditions with components of axial vorticity. The jet then exhausts into a quiescent surrounding. The present investigation is concerned with injection into a crossflow for use in gas turbine combustors where multijet arrangements would be used for modification of the mainstream.

Experimental

The mixing experiments were performed in a 12 × 12 cm horizontal wind tunnel with provision for jet injection through one wall as shown in Fig. 1. The air for the crossflow was supplied by a blower attached to the tunnel inlet with a 20-cm-diam flexible duct. The inlet/settling section was 43 × 43 cm and contained a dense furnace filter to distribute the flow, followed by a honeycomb and a series of two wire–mesh 50% open screens for flow conditioning. The 43 × 43 cm cross section then contracted on all four sides by a third-order polynomial to the 12 × 12 cm test section. The crossflow/mainstream velocity was set at 6.6 m/s and the velocity variation across the test section was less than 5%. Turbulence intensity was 1%.

The jet enters the tunnel through a sharp-edged (3.2-mm-thick) orifice machined into an interchangeable bottom wall. The other three walls of the test section are 3.2-mm-thick plate glass. The jet flow originates in a 10 × 10 × 12 cm plenum attached to the bottom of the test section. The mass flow into the plenum was maintained at 0.0043 kg/s using a laminar flow element.

Presented as Paper 95-0732 at the AIAA 33rd Aerospace Sciences Meeting and Exhibit, Reno, NV, Jan. 9–12, 1995; received Feb. 4, 1995; revision received April 26, 1995; accepted for publication April 26, 1995.

*Research Scientist, Chemical Sciences. Member AIAA.
†Senior Laboratory Technician, Chemical Sciences.
‡Senior Research Engineer, Internal Fluid Mechanics. Associate Fellow AIAA.

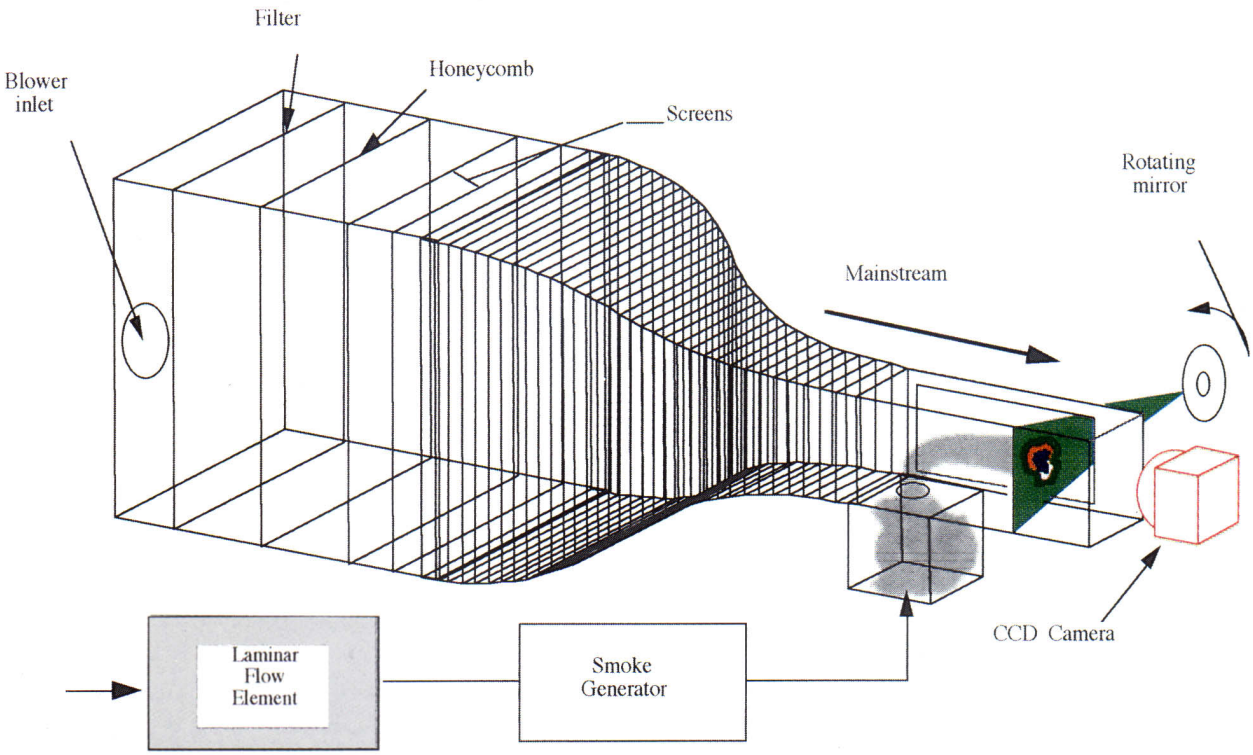

Fig. 1 Experimental configuration used to measure planar concentration distributions.

Table 1 Sharp-edge orifice configurations

Configuration	Orifice shape	Width × length, cm × cm	AR	α
A	y, x	1.91 × 1.91	1:1	0
B		1.69 × 1.69	1:1	0
C		1.35 × 2.70	2:1	0
D		2.70 × 1.35	2:1	90
E		1.27 × 2.54	2:1	0
F		2.54 × 1.27	2:1	90

Table 1 identifies the six orifice configurations that were tested. Note that configurations C and D and E and F are the same orifice shape rotated 90 deg. The physical area of each orifice was 2.86 cm^2. Discharge coefficients C_d were measured in a separate apparatus for each orifice plate at the mass flow rate used in the investigation. The C_d of each plate was found to be 0.67 resulting in a bulk jet velocity of 19 m/s. The jet-to-mainstream momentum-flux ratio J was 8.2. This J was chosen so that the jets would have a trajectory that roughly followed the midpoint of the tunnel and avoided wall contact. The Reynolds number of the jet was typically 2.4×10^4.

Mie scattering was the primary diagnostic used to optically measure jet mixture fraction distributions in planes parallel and perpendicular to the duct axis. The planar digital imaging technique (see Refs. 12 and 26) is applied by marking the jet flow with an oil aerosol (micrometer-size particles). A light sheet (0.5 mm thick) is created using 2-W argon–ion laser and a rotating mirror. The flowfield was illuminated to acquire planes oriented in either 1) a side view, by passing the light sheet through the orifice centerline in the axial direction or 2) the end-on view, by passing the light sheet through planes perpendicular to the injection wall (y–z plane) at various axial locations. An image-intensified thermoelectrically cooled charge-coupled device (CCD) camera fitted with standard 35-mm lenses was used to record the scattered light intensity. For the side views the camera was focused through the side window on the illuminated plane. For the end-on view the camera was located inside the duct 61-cm downstream of the orifice midpoint. The camera was programmed to make exposures coincident with the sweep of the beam through the flowfield. The mean concentration distributions were acquired over 15 s and represent the time-average intensity of about 2000 instantaneous distributions that were then digitized in a 380 × 380 pixel format (pixel size = 0.3 × 0.3 × 0.5 mm) and sent to a computer for storage. The scattered light intensity is proportional to the number of particles in the measurement volume. If only one of two streams is marked (in this study the jet fluid), the light intensity of the undiluted marked fluid represents mole fraction unity.

In addition to the optical measurements, a series of gas-sampling probe measurements was made to provide independent calibration of the Mie scattering distributions. A methane tracer was introduced into the jet fluid and a total hydrocarbon analyzer was used to detect the methane. For those measurements a 3.2-mm-diam stainless steel probe was mounted on a platform that could be moved both vertically and horizontally. While the downstream location (x direction) was positioned manually, a stepper motor moved the probe in 3.2-mm increments throughout the y–z plane under computer control. A delay of 2 s at each station was sufficient to purge the sample line. The on-line total hydrocarbon analyzer continuously measured the methane concentration that was compared with the reference concentration to obtain a jet mixture fraction at 1369 data points.

Mean flow velocity in the streamwise direction and the rms value were obtained using a linearized constant temperature

hot-wire anemometer. A single wire oriented perpendicular to the mainstream flow was traversed in a fashion similar to the gas-sampling probe described in the previous paragraph. Average quantities were recorded at 440 points/plane and turbulence intensity is reported. The probe orientation was not varied, therefore, only velocity components in the streamwise direction were measured. Although the probe response was 13 kHz, spectra were not recorded.

Results and Discussion

Mean concentration distributions for the six orifice configurations are shown in Fig. 2. The distributions are side views, the x–z plane bisecting the orifice and parallel to the mainstream flow direction. A 10-level color scale is used to represent contours of jet mass fraction from 0 to 1.0 (pure mainstream fluid colored red = 0 and pure jet fluid colored dark blue = 1.0, note that the acquired data has a resolution several orders of magnitude greater than that displayed by the contour plot). Mainstream flow is from left-to-right and the jet obviously enters from the bottom left. A plan view of the orifice shape is displayed in the upper left corner. The images are cropped so that the left side begins at $x = 0$, the leading edge of the orifice, and the right side is at $x/d = 5.5$ (where d = the diameter of an equivalent area circle).

The white line through each figure, which starts at the orifice midpoint and bends with the jet, is the same in each of the six plots. It corresponds to the trajectory of the round orifice, i.e., configuration A. Trajectory is defined as the line that intersects the maximum jet concentration as a function of downstream distance. The black line plotted on the round orifice data (configuration A) is the trajectory predicted by an empirical correlation reported by Holdeman[27] for the centerplane temperature trajectory of a single heated jet in crossflow:

$$z/d = 0.76(\rho_j/\rho_m)^{0.15} J^{0.52} (x/d)^{0.27} \quad (1)$$

The observed trajectory bends more quickly than the prediction, but overall the agreement is good. All of the configurations except C and E are quite similar in trajectory and overall flow features. Configurations C and E are slightly different in trajectory and in the wake region directly behind the jet. These configurations have slower mass addition due to their longer axial length. If the origin of the trajectory curve was moved nearer to the leading edge, instead of at the orifice midpoint, the same trajectory curve would closely approximate all of the configurations.

To study mixing performance, end-on views (planar cross sections of the flowfield perpendicular to the mainstream flow direction) were acquired at several downstream locations for each orifice configuration. In Fig. 3 the jet mixture fraction distributions of the configurations shown in Table 1 are compared at four downstream positions using a 10-color contour plot to represent jet mixture fraction. In these plots only the jet/mainstream mixing region is shown. The downstream position is indicated on the figure as a nondimensionalized distance where the axial distance is normalized by the orifice diameter x/d. For the noncircular orifices the equivalent round orifice diameter is used for normalization. The primary difference between the distributions is the rate of development of the counter-rotating vortices. The development is the most rapid in configurations C and E, the aligned ellipse and aligned slot, respectively, followed by the circle, square, and transverse ellipse and slot. It is surprising that although the development of vorticity appears to be quite different, the overall degree of mainstream entrainment, i.e., mixing performance, appears to be similar in each case. Apparently, although low mainstream blockage increases the degree of counter-rotating vorticity, the slower mass addition rate is offsetting. Therefore, the net

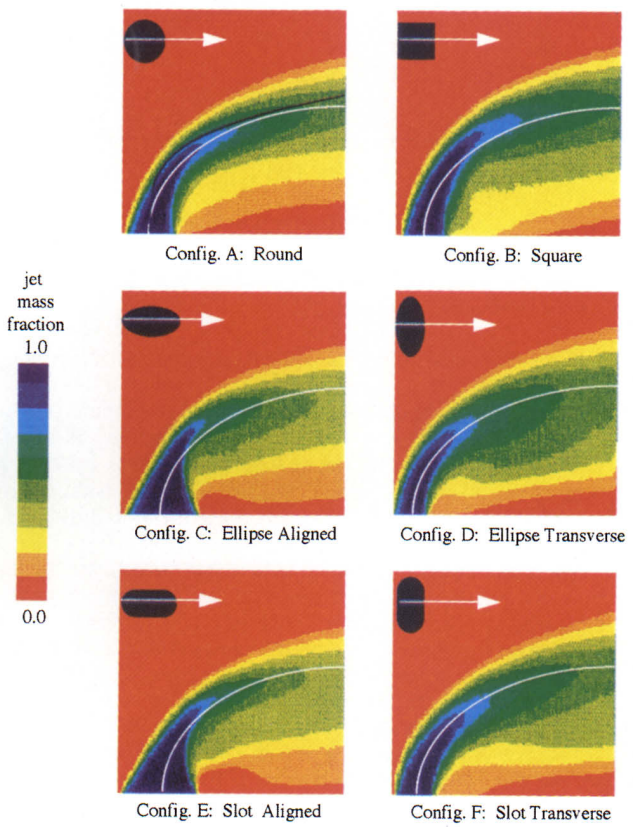

Fig. 2 Side view of the average jet mixture fraction distribution for the six orifice configurations in Table 1 (left side of each figure is x/d = 0, right side is x/d = 5.5, where d is the diameter of an equivalent area circle).

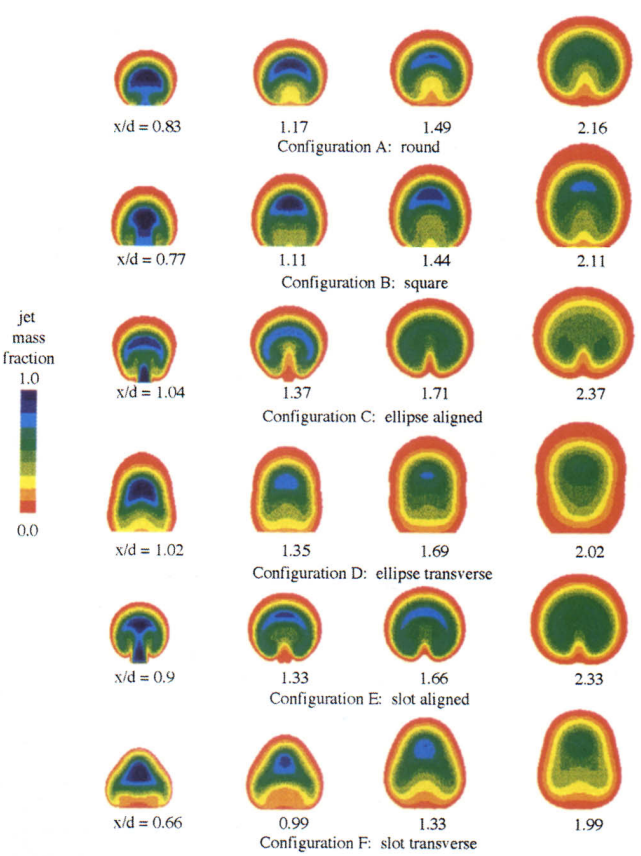

Fig. 3 Comparison of end-on jet mixture fraction distributions (axial locations are nondimensionalized by d, the equivalent round orifice diameter).

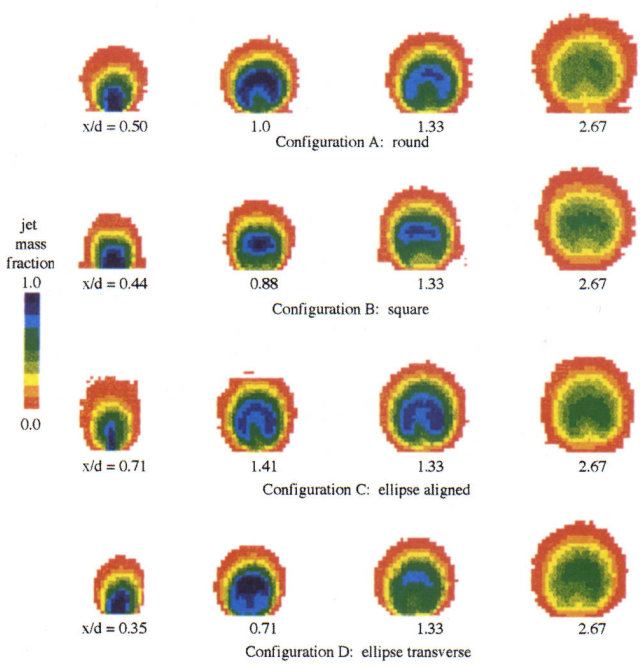

Fig. 4 Comparison of jet mixture fraction distributions (gas sampling) (axial locations are nondimensionalized by *d*, the equivalent round orifice diameter).

entrainment as a function of downstream distance is equivalent.

The results of the methane tracer analysis are shown in Fig. 4 for the first four orifice configurations. The plotting is the same as in Fig. 3. Note the spatial resolution is very coarse, but the overall qualities of the flowfield are still apparent. In general, the agreement of the two data sets is very good. The ordering of development of vorticity is shown to be the same and the net mixing performance is seen to be quite similar.

In a two-stream mixing problem the fully mixed concentration is defined by the jet-to-mainstream mass-flow ratio. A measure of the mixing rate can be obtained by comparing the jet mixture fraction distribution at any downstream plane to the fully mixed value. In Ref. 11 the authors developed a measure of unmixedness based on the variance of the concentration distribution, defined as spatial unmixedness:

$$U_s = \frac{c_{\text{var}}}{c_{\text{av}}(1 - c_{\text{av}})} \tag{2}$$

where

$$c_{\text{var}} = \frac{1}{m}\sum_{i=1}^{m} (\bar{c}_i - c_{\text{av}})^2 = \text{spatial concentration variance}$$

$$\bar{c}_i = \text{time-average concentration at a pixel}$$

$$c_{\text{av}} = \text{fully mixed concentration}$$

$U_s = 0$ corresponds to a perfectly mixed system and $U_s = 1$ corresponds to a perfectly segregated system. The denominator is the maximum concentration fluctuation that can occur at the specified fully mixed concentration. Normalizing by this factor allows U_s values to be compared regardless of the jet-to-mainstream mass flow ratio of the system. Therefore, this parameter allows comparison of the relative mixing effectiveness of each configuration reported herein and comparison to other configurations with different mass flow ratios, where

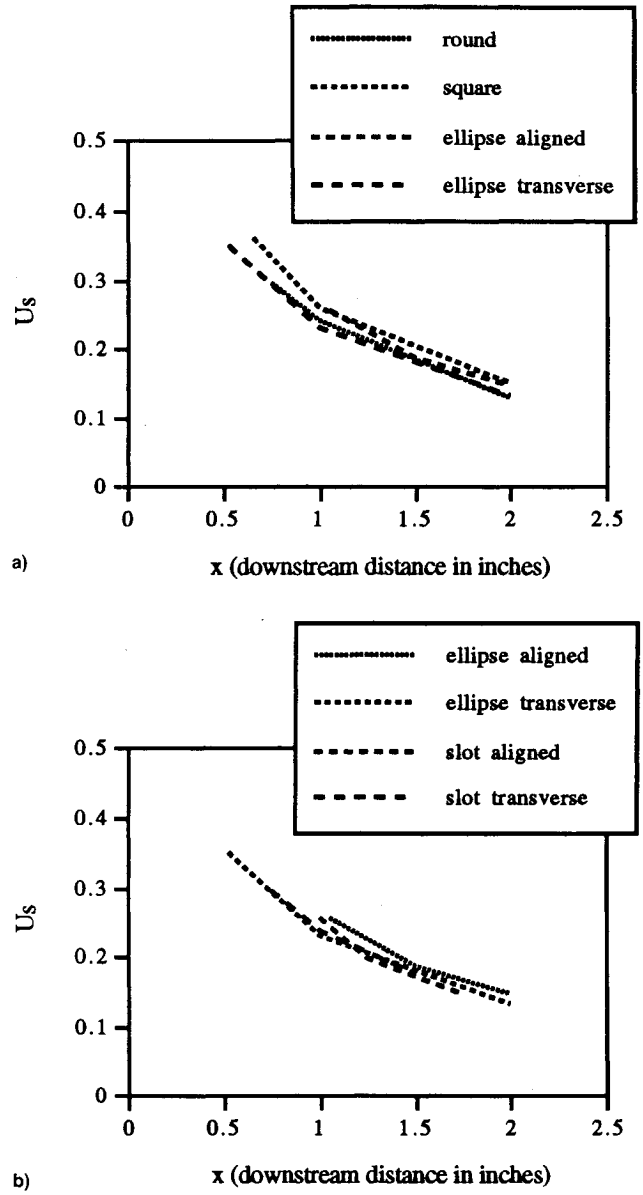

Fig. 5 Comparison of the spatial unmixedness of a) circular and noncircular orifices (configurations A–D) and b) elliptical and slot orifices (configurations C–F).

d = the diameter of an equivalent area circle, i.e., multijet arrangements.

Spatial unmixedness as a function of downstream position for the configurations in Table 1 is shown in Figs. 5a and 5b. These curves agree with the conclusions reached by comparison of the distributed shown in Figs. 3 and 4. Although the mixing rates are slightly different, they are not substantially different.

To further characterize the flowfield and investigate the fluctuating properties, a hot-wire anemometer was used to measure the turbulence intensity in the streamwise direction at several downstream planes for all of the configurations in Table 1. Turbulence intensity is defined as the (rms velocity)/(mean velocity). In Fig. 6 the results are presented as contour plots where red represents the highest fluctuations (60%) and black the lowest. The figures represent 6.4 × 6.4 cm areas centered around the orifice with the bottom of the figure starting at the injection plane ($z = 0$).

At the first downstream station, which is a plane through the midpoint of the orifice, the highest levels, which are about 20%, are at the interface of the jet and mainstream. Fluctuations in the core regions directly above the jet are low. The

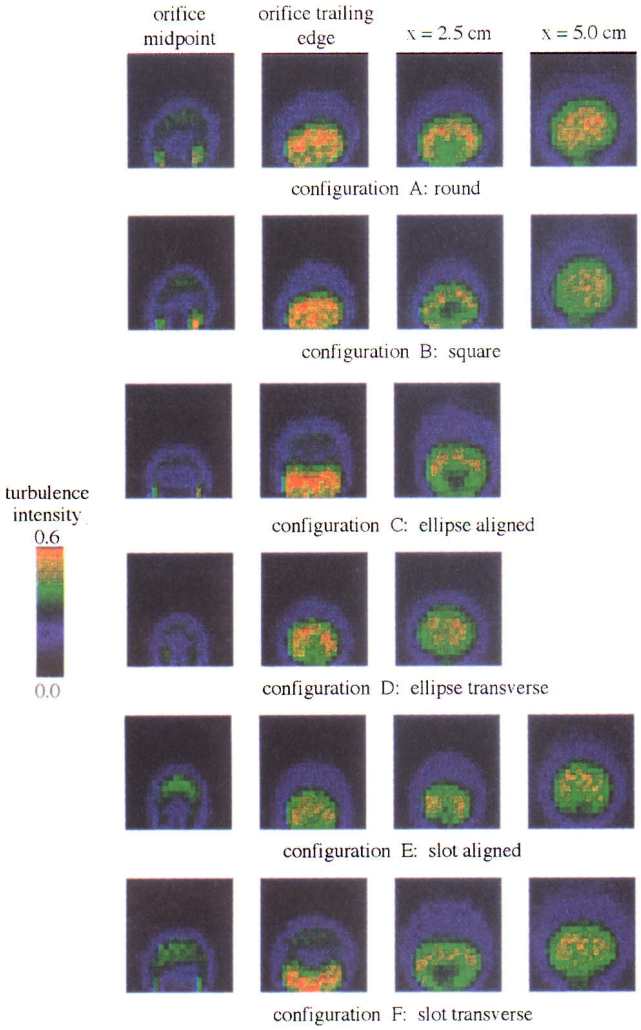

Fig. 6 Turbulence intensity distributions for the six orifice configurations in Table 1.

levels and distributions are independent of the configuration. At the trailing edge very high levels are indicated in the wake region for each configuration. Since only a single velocity component was resolved, these measurements are probably biased by intermittency and recirculation in that region. Farther downstream at the 2.5- and 5-cm locations the distributions become symmetric about the orifice midpoint and the highest fluctuations are now centered in the plume of the jet. It is surprising that the overall agreement between the configurations is so similar. This would indicate that on average each of the configurations generates similar vorticity in the streamwise direction. The result is consistent with the similarity in entrainment rates indicated by the concentration distributions.

Conclusions

1) Based on the mean concentration distributions, turbulent mixing was not affected significantly by orifice shape.

2) Mean concentration trajectories are similar independent of orifice shape.

3) Concentration distributions are similar whether measured by Mie scattering or by probes.

4) Measurements of turbulence intensity indicated that the distribution and level of fluctuation were similar for each shape.

5) More detailed analysis using multicomponent hot wires to resolve the three-dimensional flowfield are necessary to determine the effect of orifice shape on turbulence length scales. Spectra and cross correlations are necessary.

Acknowledgments

This work was supported by NASA Contract NAS3-25954, Task Order no. 12. The assistance of Brian Knight of UTRC with the hot-wire anemometry is gratefully acknowledged.

References

[1]Bain, D. B., Smith, C. E., and Holdeman, J. D., "CFD Assessment of Orifice Aspect Ratio and Mass Flow Ratio on Jet Mixing in Rectangular Ducts," AIAA Paper 94-0218, Jan. 1994; also NASA TM 106434, Jan. 1994.

[2]Bain, D. B., Smith, C. E., and Holdeman, J. D., "Mixing Analysis of Axially Opposed Rows of Jets Injected into Confined Crossflow," *Journal of Propulsion and Power*, Vol. 11, No. 5, 1995, pp. 885–893; also NASA TM 106179, June 1993.

[3]Bain, D. B., Smith, C. E., and Holdeman, J. D., "CFD Mixing Analysis of Jets Injected from Straight and Slanted Slots into Confined Crossflow in Rectangular Ducts," AIAA Paper 92-3087, July 1992; also NASA TM 105699, July 1992.

[4]Doerr, T., and Hennecke, D. K., "The Mixing Process in the Quenching Zone of the Rich-Lean Combustion Concept," AGARD-PEP 81st Symposium of Fuels and Combustion Technology for Advanced Aircraft Engines, 1993.

[5]Hatch, M. S., Sowa, W. A., Samuelsen, G. S., and Holdeman, J. D., "Geometry and Flow Influences on Jet Mixing in a Cylindrical Duct," *Journal of Propulsion and Power*, Vol. 11, No. 3, 1995, pp. 393–402; also AIAA Paper 92-0773, Jan. 1992; NASA TM 105390, Jan. 1992.

[6]Hatch, M. S., Sowa, W. A., Samuelsen, G. S., and Holdeman, J. D., "Influence of Geometry and Flow Variations on NO Formation in the Quick Mixer of a Staged Combustor," *Journal of Engineering for Gas Turbines and Power*, to be published; also NASA TM 105639, July 1992.

[7]Holdeman, J. D., "Mixing of Multiple Jets with a Confined Subsonic Crossflow," *Progress in Energy and Combustion Science*, Vol. 19, 1993, pp. 31–70; also AIAA Paper 91-2458, June 1991, and NASA TM 104412.

[8]Howe, G. W., Li, Z., Shih, T. I-P., and Nguyen, H. L., "Simulation of Mixing in the Quick Quench Region of a Rich Burn–Quick Quench Mix–Lean Burn Combustor," AIAA Paper 91-0410, Jan. 1991.

[9]Kroll, J. T., Sowa, W. A., Samuelson, G. S., and Holdeman, J. D., "Optimization of Circular Orifice Jets Mixing into a Heated Crossflow in a Cylindrical Duct," AIAA Paper 93-0249, Jan. 1993; also NASA TM 105984, Jan. 1993.

[10]Liscinsky, D. S., True, B., and Holdeman, J. D., "Mixing Characteristics of Directly Opposed Rows of Jets Injected Normal to a Cross flow in a Rectangular Duct," AIAA Paper 94-0217, Jan. 1994; also NASA TM 106477, Jan. 1994.

[11]Liscinsky, D. S., True, B., and Holdeman, J. D., "Experimental Investigation of Crossflow Jet Mixing in a Rectangular Duct," AIAA Paper 93-2037, June 1993; also NASA TM 106152, June 1993.

[12]Liscinsky, D. S., True, B., Vranos, A., and Holdeman, J. D., "Experimental Study of Cross-Stream Mixing in a Rectangular Duct," AIAA Paper 92-3090, July 1992; also NASA TM 106194, July 1992.

[13]Oechsle, V. L, Mongia, H. C., and Holdeman, J. D., "Comparison of the Mixing Calculations of the Reacting and Nonreacting Flows in a Cylindrical Duct," AIAA Paper 94-0865, Jan. 1994; also NASA TM 106435, Jan. 1994.

[14]Oechsle, V. L., Mongia, H. C., and Holdeman, J. D. "An Analytical Study of Jet Mixing in a Cylindrical Duct," AIAA Paper 93-2043, June 1993; also NASA TM 106181, June 1993.

[15]Oechsle, V. L., Mongia, H. C., and Holdeman, J. D., "A Parametric Numerical Study of Mixing in a Cylindrical Duct," AIAA Paper 92-3088, July 1992; also NASA TM 105695, July 1992.

[16]Smith, C. E., Talpallikar, M. V., and Holdeman, J. D., "A CFD Study of Jet Mixing in Reduced Areas for Lower Combustor Emissions," AIAA Paper 91-2460, June 1991; also NASA TM 104411, June 1991.

[17]Sowa, W. A., Kroll, J. T., Samuelsen, G. S., and Holdeman, J. D., "Optimization of Orifice Geometry for Cross-Flow Mixing in a Cylindrical Duct," AIAA Paper 94-0219, Jan. 1994; also NASA TM

106436, Jan. 1994.

[18]Talpallikar, M. V., Smith, C. E., Lai, M. C., and Holdeman, J. D., "CFD Analysis of Jet Mixing in Low NOx Flametube Combustors," *Journal of Engineering for Gas Turbines and Power*, Vol. 114, 1992, p. 416; also American Society of Mechanical Engineers, ASME 91-217 and NASA TM 104466, June 1991.

[19]Vranos, A., Liscinsky, D. S., True, B., and Holdeman, J. D., "Experimental Study of Cross-Stream Mixing in a Cylindrical Duct," AIAA Paper 91-2459, June 1991; also NASA TM 105180.

[20]Zhu, G., and Lai, M.-C., "A Parametric Study of Penetration and Mixing of Radial Jets in Necked-Down Cylindrical Cross-Flow," AIAA Paper 92-3091, July 1992.

[21]Ho, C.-M., and Gutmark, E., "Vortex Induction and Mass Entrainment in a Small-Aspect-Ratio Elliptic Jet," *Journal of Fluid Mechanics*, Vol. 179, 1987, pp. 383–405.

[22]Gutmark, E., and Ho, C.-M., "Visualization of a Forced Elliptic Jet, *AIAA Journal*, Vol. 24, No. 4, 1986, pp. 684, 685.

[23]Gutmark, E., and Schadow, K. C., "Flow Characteristics of Orifice and Tapered Jets," *Physics of Fluids*, Vol. 30, No. 11, 1987, pp. 3448–3454.

[24]Quinn, W. R., "On Mixing in an Elliptic Turbulent Free Jet," *Physics of Fluids*, Vol. A1, No. 10, 1989, pp. 1716–1722.

[25]Wu, J. M., Vakili, A. D., and Yu, F. M., "Investigation of the Interacting Flow of Nonsymmetric Jets in Crossflow," *AIAA Journal*, Vol. 26, No. 8, 1988, pp. 940–947.

[26]Liscinsky, D. S., and True, B., "Planar Mie Scattering Measurements of Scalar Mixing," *SPIE Proceedings*, Vol. 2122-18, Society of Photo-Optical Instrumentation Engineers, Jan. 1994, pp. 153–160.

[27]Holdeman, J. D., "Correlation for Temperature Profiles in the Plane of Symmetry Downstream of a Jet Injected Normal to a Crossflow," NASA TN D-6966 Sept. 1972.